

# JES

JOURNAL OF  
ENVIRONMENTAL  
SCIENCES

April 1, 2015 Volume 30  
[www.jesc.ac.cn](http://www.jesc.ac.cn)

ISSN 1001-0742  
CN 11-2629/X



## MBR in Wastewater Reclamation



Sponsored by  
Research Center for Eco-Environmental Sciences  
Chinese Academy of Sciences

**Highlight articles**

- 129 Rice: Reducing arsenic content by controlling water irrigation  
Ashley M. Newbigging, Rebecca E. Paliwoda and X. Chris Le
- 132 Apportioning aldehydes: Quantifying industrial sources of carbonyls  
Sarah A. Styler

**Review articles**

- 30 Application of constructed wetlands for wastewater treatment in tropical and subtropical regions (2000-2013)  
Dong-Qing Zhang, K.B.S.N. Jinadasa, Richard M. Gersberg, Yu Liu, Soon Keat Tan and Wun Jern Ng
- 47 Stepwise multiple regression method of greenhouse gas emission modeling in the energy sector in Poland  
Alicja Kolasa-Wiecek
- 113 Mini-review on river eutrophication and bottom improvement techniques, with special emphasis on the Nakdong River  
Andinet Tekile, Ilho Kim and Jisung Kim

**Regular articles**

- 1 Effects of temperature and composite alumina on pyrolysis of sewage sludge  
Yu Sun, Baosheng Jin, Wei Wu, Wu Zuo, Ya Zhang, Yong Zhang and Yaji Huang
- 9 Numerical study of the effects of local atmospheric circulations on a pollution event over Beijing-Tianjin-Hebei, China  
Yucong Miao, Shuhua Liu, Yijia Zheng, Shu Wang and Bicheng Chen, Hui Zheng and Jingchuan Zhao
- 21 Removal kinetics of phosphorus from synthetic wastewater using basic oxygen furnace slag  
Chong Han, Zhen Wang, He Yang and Xiangxin Xue
- 55 Abatement of SO<sub>2</sub>-NO<sub>x</sub> binary gas mixtures using a ferruginous active absorbent: Part I. Synergistic effects and mechanism  
Yinghui Han, Xiaolei Li, Maohong Fan, Armistead G. Russell, Yi Zhao, Chunmei Cao, Ning Zhang and Genshan Jiang
- 65 Adsorption of benzene, cyclohexane and hexane on ordered mesoporous carbon  
Gang Wang, Baojuan Dou, Zhongshen Zhang, Junhui Wang, Haier Liu and Zhengping Hao
- 74 Flux characteristics of total dissolved iron and its species during extreme rainfall event in the midstream of the Heilongjiang River  
Jiunian Guan, Baixing Yan, Hui Zhu, Lixia Wang, Duian Lu and Long Cheng
- 81 Sodium fluoride induces apoptosis through reactive oxygen species-mediated endoplasmic reticulum stress pathway in Sertoli cells  
Yang Yang, Xinwei Lin, Hui Huang, Demin Feng, Yue Ba, Xuemin Cheng and Liuxin Cui
- 90 Roles of SO<sub>2</sub> oxidation in new particle formation events  
He Meng, Yujiao Zhu, Greg J. Evans, Cheol-Heon Jeong and Xiaohong Yao
- 102 Biological treatment of fish processing wastewater: A case study from Sfax City (Southeastern Tunisia)  
Meryem Jemli, Fatma Karray, Firas Feki, Slim Loukil, Najla Mhiri, Fathi Aloui and Sami Sayadi

## CONTENTS

- 122 Bioreduction of vanadium (V) in groundwater by autohydrogentrophic bacteria: Mechanisms and microorganisms  
Xiaoyin Xu, Siqing Xia, Lijie Zhou, Zhiqiang Zhang and Bruce E. Rittmann
- 135 Laccase-catalyzed bisphenol A oxidation in the presence of 10-propyl sulfonic acid phenoxazine  
Rūta Ivanec-Goranina, Juozas Kulys, Irina Bachmatova, Liucija Marcinkevičienė and Rolandas Meškys
- 140 Spatial heterogeneity of lake eutrophication caused by physiogeographic conditions: An analysis of 143 lakes in China  
Jingtao Ding, Jinling Cao, Qigong Xu, Beidou Xi, Jing Su, Rutai Gao, Shouliang Huo and Hongliang Liu
- 148 Anaerobic biodegradation of PAHs in mangrove sediment with amendment of  $\text{NaHCO}_3$   
Chun-Hua Li, Yuk-Shan Wong, Hong-Yuan Wang and Nora Fung-Yee Tam
- 157 Achieving nitrification at low temperatures using free ammonia inhibition on *Nitrobacter* and real-time control in an SBR treating landfill leachate  
Hongwei Sun, Yongzhen Peng, Shuying Wang and Juan Ma
- 164 Kinetics of Solvent Blue and Reactive Yellow removal using microwave radiation in combination with nanoscale zero-valent iron  
Yanpeng Mao, Zhenqian Xi, Wenlong Wang, Chunyuan Ma and Qinyan Yue
- 173 Environmental impacts of a large-scale incinerator with mixed MSW of high water content from a LCA perspective  
Ziyang Lou, Bernd Bilitewski, Nanwen Zhu, Xiaoli Chai, Bing Li and Youcai Zhao
- 180 Quantitative structure-biodegradability relationships for biokinetic parameter of polycyclic aromatic hydrocarbons  
Peng Xu, Wencheng Ma, Hongjun Han, Shengyong Jia and Baolin Hou
- 191 Chemical composition and physical properties of filter fly ashes from eight grate-fired biomass combustion plants  
Christof Lanzerstorfer
- 198 Assessment of the sources and transformations of nitrogen in a plain river network region using a stable isotope approach  
Jingtao Ding, Beidou Xi, Qigong Xu, Jing Su, Shouliang Huo, Hongliang Liu, Yijun Yu and Yanbo Zhang
- 207 The performance of a combined nitrification-anammox reactor treating anaerobic digestion supernatant under various C/N ratios  
Jian Zhao, Jiane Zuo, Jia Lin and Peng Li
- 215 Coagulation behavior and floc properties of compound bioflocculant-polyaluminum chloride dual-coagulants and polymeric aluminum in low temperature surface water treatment  
Xin Huang, Shenglei Sun, Baoyu Gao, Qinyan Yue, Yan Wang and Qian Li
- 223 Accumulation and elimination of iron oxide nanomaterials in zebrafish (*Danio rerio*) upon chronic aqueous exposure  
Yang Zhang, Lin Zhu, Ya Zhou and Jimiao Chen
- 231 Impact of industrial effluent on growth and yield of rice (*Oryza sativa* L.) in silty clay loam soil  
Mohammad Anwar Hossain, Golum Kibria Muhammad Mustafizur Rahman, Mohammad Mizanur Rahman, Abul Hossain Molla, Mohammad Mostafizur Rahman and Mohammad Khabir Uddin
- 241 Molecular characterization of microbial communities in bioaerosols of a coal mine by 454 pyrosequencing and real-time PCR  
Min Wei, Zhisheng Yu and Hongxun Zhang
- 252 Risk assessment of *Giardia* from a full scale MBR sewage treatment plant caused by membrane integrity failure  
Yu Zhang, Zhimin Chen, Wei An, Shumin Xiao, Hongying Yuan, Dongqing Zhang and Min Yang
- 186 Serious BTEX pollution in rural area of the North China Plain during winter season  
Kankan Liu, Chenglong Zhang, Ye Cheng, Chengtang Liu, Hongxing Zhang, Gen Zhang, Xu Sun and Yujing Mu

Available online at [www.sciencedirect.com](http://www.sciencedirect.com)

ScienceDirect

[www.journals.elsevier.com/journal-of-environmental-sciences](http://www.journals.elsevier.com/journal-of-environmental-sciences)

**JES**  
JOURNAL OF  
ENVIRONMENTAL  
SCIENCES  
[www.jesc.ac.cn](http://www.jesc.ac.cn)

# Kinetics of Solvent Blue and Reactive Yellow removal using microwave radiation in combination with nanoscale zero-valent iron

Yanpeng Mao<sup>1</sup>, Zhenqian Xi<sup>1</sup>, Wenlong Wang<sup>1</sup>, Chunyuan Ma<sup>1</sup>, Qinyan Yue<sup>2,\*</sup>

1. School of Energy and Power Engineering, Shandong University, Jinan 250100, China. E-mail: [maoyanpeng@sdu.edu.cn](mailto:maoyanpeng@sdu.edu.cn)

2. School of Environmental Science and Engineering, Shandong University, Jinan 250100, China

## ARTICLE INFO

### Article history:

Received 11 June 2014

Revised 8 September 2014

Accepted 10 September 2014

Available online 30 January 2015

### Keywords:

Microwave

nZVI

Dye

Efficiency

Kinetics

## ABSTRACT

We investigated the efficiency and kinetics of the degradation of soluble dyes over the pH range 5.0–9.0 using a method employing microwave radiation in combination with nanoscale zero-valent iron (MW-nZVI). The nZVI particles (40–70 nm in diameter) were prepared by a liquid-phase chemical reduction method employing starch as a dispersant. Compared to the removal of Solvent Blue 36 and Reactive Yellow K-RN using only nZVI, more rapid and efficient dye removal and total organic carbon removal were achieved using MW-nZVI. The dye removal efficiency increased significantly with decreasing pH, but was negligibly affected by variation in the microwave power. The kinetics of dye removal by MW-nZVI followed both an empirical equation and the pseudo first-order model, while the kinetics of dye removal using nZVI could only be described by an empirical equation. It was also concluded that microwave heating of the dye solutions as well as acceleration of corrosion of nZVI and consumption of Fe(II) were possible reasons behind the enhanced dye degradation.

© 2015 The Research Center for Eco-Environmental Sciences, Chinese Academy of Sciences.

Published by Elsevier B.V.

## Introduction

Textile dyeing and processing is one of the pillar industries of China, especially the Shandong Province, which is located on the eastern line of the South-to-North Water Transfer Project of China. Therefore, strict water pollutant discharge standard DB37/599-2006 (Shandong Environmental Protection Agency, 2006) must be adhered to by the textile factories located in this region to avoid enforced discontinuation of production by the government agencies. Moreover, the textile dyes commonly used in the textile industry exhibit anti-oxidation and anti-photodecomposition properties, and give high-strength chemical oxygen demand (COD) and high chroma wastewater (Tichonovas et al., 2013), making the decolorization of dyeing wastewater much more difficult, thus leading to considerable environmental impact on surface water (Comparelli et al., 2005; Gupta et al., 2012; Krissanasraerane et al., 2010). Hence, a rapid and

efficient technique for dye removal is not only desirable but also imperative for the survival of textile factories located along the eastern line and the water security of the Water Transfer Project.

Over the past few decades, degradation of dyes by zero-valent iron (ZVI) particles, especially nanoscale ZVI (nZVI), has emerged as one of the latest innovative technologies for dye wastewater treatment and environmental remediation (Bigg and Judd, 2001; Bokare et al., 2008; Cao et al., 1999; Chang et al., 2006; Epolito et al., 2008; Fan et al., 2009; Feng et al., 2000; Lin et al., 2008; Liu et al., 2007; Mu et al., 2004; Nam and Tratnyek, 2000; Perey et al., 2002; Shu et al., 2007, 2010; Zhang et al., 2005). In addition to the application of ZVI or nZVI to dye wastewater treatment, combinations of ZVI with various methods have also been attempted. Recently, microwave (MW) assisted methods such as MW-UV (Horikoshi et al., 2002, 2004b), MW-Fenton (Gromboni et al., 2007), MW-H<sub>2</sub>O<sub>2</sub> (Klán and Vavrik, 2006; Prasannakumar et al., 2009), and

\* Corresponding author. E-mail: [qyyue58@aliyun.com](mailto:qyyue58@aliyun.com) (Qinyan Yue).



MW-K<sub>2</sub>S<sub>2</sub>O<sub>8</sub> (Lee et al., 2009) have gained popularity, as indicated by numerous publications (Remya and Lin, 2011a). These studies concluded that MW radiation could enhance the efficiency of advanced oxidation processes for the degradation of organic pollutants (Gromboni et al., 2007; Yang et al., 2009; Zhang et al., 2007; Zhanqi et al., 2007).

The removal of organics using MW radiation in combination with ZVI and nZVI (henceforth denoted as MW-ZVI or MW-nZVI) has also gained interest in the last few years, because it provides fast and effective degradation of organic wastewater without abiotic reduction and oxidant dosage. Oh et al. (2006) reported first that 98% of perchlorate in water was removed by cast iron in 1 hr via microwave heating at pH 7.4. Jou (2008) degraded 1000 mg/L of pentachlorophenol using 700 W MW power and 0.5 g/L ZVI, achieving a removal efficiency exceeding 99% in 30 sec. Lee et al. (2010) reported that MW-nZVI could reduce the chlorobenzene activation energy by 6.1 kJ/mol and increase chlorobenzene removal efficiency 4.1 times. Furthermore, Lee and Jou (2012) found that nZVI with the application of MW radiation had greater ability to reduce the chlorobenzene activation energy than commercial micron-sized iron particles. Fu et al. (2010) developed a novel method of zero-valent iron/activated carbon combined with microwave discharge electrodeless lamp/sodium hypochlorite to remove Reactive Red 195, and obtained 100% color removal efficiency and 82% COD removal efficiency. Remya and Lin (2011b) found that complete carbofuran degradation could be accomplished in 5 min by MW-ZVI at pH 10 and 80°C.

The removal of dye from wastewater is a major concern, especially in the sensitive area along the South-to-North Water Transfer project of China. Although it has been accepted that MW-nZVI is a highly efficient method for the removal of organics, to the best of our knowledge, the removal of Solvent Blue 36 and Reactive Yellow K-RN from aqueous solution by MW-nZVI has not been reported previously. Hence, to advance our understanding of the reduction of dyes in the environment, we designed various aqueous systems to investigate the kinetics of the removal of these two dyes via MW-nZVI. The effects of key parameters including nZVI dosage, initial pH, and temperature on the dyes removal were examined to study the removal kinetics.

## 1. Materials and methods

### 1.1. Materials

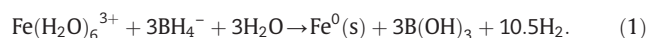
Analytical grade reagents were used in all cases (except when noted) and were purchased from Shanghai Chemical Reagents Company, Shanghai, China. Organic dyes, namely, Solvent Blue 36 (C<sub>20</sub>H<sub>22</sub>N<sub>2</sub>O<sub>2</sub>, purity: ≥98%) and Reactive Yellow K-RN (C<sub>21</sub>H<sub>17</sub>ClN<sub>8</sub>O<sub>7</sub>S<sub>2</sub>, purity: ≥98%), which were obtained from Liaocheng Sanhe Textile Co., Ltd., Shandong, China, were used without any purification as the target contaminants. The molecular structures of these organic dyes are shown in Fig. 1. All solutions were prepared using 18 MΩ cm ultrapure Milli-Q water (MQ) and stored in the dark at 4°C when not in use. All glassware and plastic ware were soaked in 5% (V/V) HCl for several days and rinsed thoroughly with MQ before use. All experiments were performed under conditions in which exposure to light was minimized by wrapping the reaction vessel with a dark cloth.

A background solution containing 2.0 mmol/L NaHCO<sub>3</sub> and 0.1 mol/L NaCl was prepared one week prior to the commencement of each experiment to ensure that equilibrium between the background solution and the atmosphere was reached. 0.1 mol/L Fe(III) solution, 0.16 mol/L NaBH<sub>4</sub> solution, 50 mg/L Solvent Blue 36 (hereafter, Blue) stock solution and 60 mg/L Reactive Yellow

K-RN (hereafter, Yellow) stock solution were prepared prior to use. Starch was vacuum-dried for 6 hr at 50°C before use.

### 1.2. Preparation of nanoscale zero-valent iron

The nZVI particles were prepared based on a liquid-phase chemical reduction method (Joo et al., 2004; Wang and Zhang, 1997). However, starch was added to the 0.1 mol/L Fe(III) solution as the dispersant, using an starch-to-iron mass ratio of 0.65:1. To fabricate sufficient nZVI particles for the dye-removal experiments, 500 mL of a mixed solution of Fe(III) and starch was placed into a 1 L conical flask for each experiment, and N<sub>2</sub> was then pumped into the solution for 3 hr to eliminate O<sub>2</sub>. In the next step, the 0.16 mol/L NaBH<sub>4</sub> solution was dropped into the reaction vessel at a rate of 2 drops/sec using a dropping funnel. Ferric iron was then reduced and black nZVI particles were precipitated at ambient temperature under stirring, according to the following reaction:



NaBH<sub>4</sub> was continually added until no further formation of nZVI was observed. The freshly prepared nZVI was quickly collected on a 0.45-μm membrane filter by filtration under suction and was sequentially washed three times using 10<sup>-4</sup> mol/L HCl, MQ, and anhydrous ethanol for the removal of iron oxides, soluble ions, and water molecules, respectively. The wet nZVI was immediately vacuum-dried at 60°C for 6 hr. The weight of the nZVI particles produced in this way was more than 2.5 g with a consistent yield of ≥89%.

### 1.3. Kinetics of dye removal by MW-nZVI

The removal of dyes from the background solution using MW-nZVI was performed in a 2.45-GHZ MCR-3 microwave chemical reactor (Yuhua Instrument, Gongyi, Henan, China) equipped with a condenser tube and a stirring apparatus. Various amounts of nZVI were added to the 250 mL 50 mg/L Blue solution or 60 mg/L Yellow solution with varying pH (5.0, 7.0, and 9.0) in Pyrex® vessels (500 mL conical flask). The pH value was measured using a PHS-3C pH meter (Leici Instrument, Shanghai, China) combined with a glass electrode and Ag/AgCl reference. It should be noted that the pH was adjusted to the desired value without adding any buffer, because the presence of a buffer was anticipated to affect the decolorization reactions between the dyes and nZVI, though this was not proved in this study. After completion of the reactions, the pH of the dye solutions was evaluated again to confirm that there was a little change (±0.5) in the pH. In this study, the initial pH values were taken as the “true” values of the investigated solutions. After the addition of nZVI, dye solutions were immediately transported to the microwave chemical reactor and constantly stirred at 50 rpm. The microwave chemical reactor with varying output power (MP = 450, 720, and 900 W) was then switched on. Samples were removed (using a 3 mL syringe) at appropriate time intervals and immediately filtered through a 25 mm diameter 0.45 μm membrane filter. The adsorption of the dye on the filter membrane was found to be negligible. The sample temperature was measured using a thermometer, and the dye concentration was evaluated using UV-Vis spectrophotometry. In addition, the removal of Blue solution or Yellow solution using

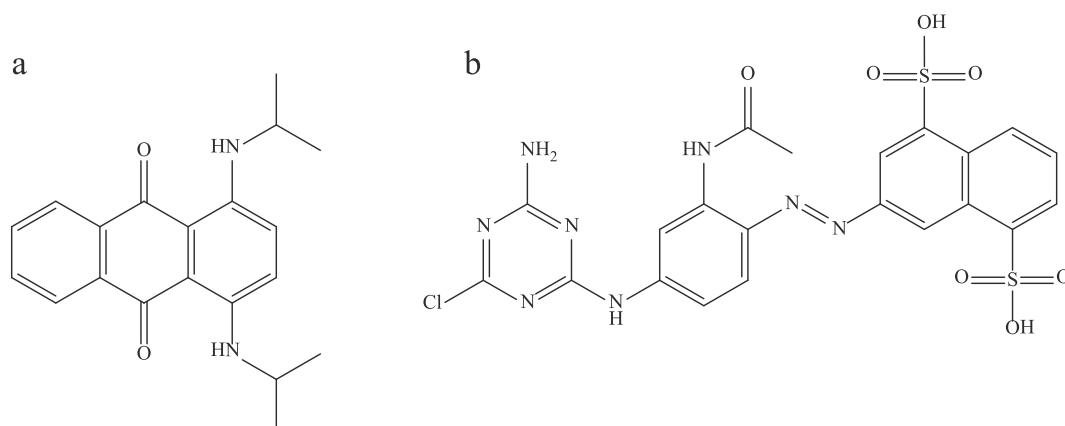


Fig. 1 – Molecular structures of Solvent Blue 36 (a) and Reactive Yellow K-RN (b).

only nZVI was performed for comparative purposes. To evaluate the effect of temperature on dye removal, we also carried out the reactions without MW in a thermostatic magnetic mixer (Yuhua Instrument, Gongyi, Henan, China) at different temperatures (25 and 70°C) controlled by a constant temperature bath; the samples were pipetted and treated in an identical manner to that described above.

#### 1.4. Chemical analysis

The specific surface areas (BET surface area) of the dry nZVI particles were measured by the nitrogen adsorption method using an Autosorb-iQ surface analyzer (Quantachrome Instruments, Boynton Beach, Florida, USA). The morphology of the particles was observed with a Tecna 20 U-twin (FEI, Hillsboro, Oregon State, USA) transmission electron microscope (TEM) at 120 kV to characterize the size and size-distribution of the metal particles. Elemental analysis of nZVI was conducted using a PW4400X-ray fluorescence (XRF, Thermo Electron Corporation, Waltham, Massachusetts, USA) spectrometer.

The concentration of dyes in the different samples was measured using a UV-Vis spectrophotometer (TU-1901, Persee, Beijing, China). From full wavelength scanning, it was found that the absorption maxima in the UV-Vis spectra of Blue solution and Yellow solution occur at 603 and 423 nm, respectively. Calibration curves (linear) for determining the dye concentrations were developed based on the absorbance signal measured using excess dye concentrations, giving rise to high  $r^2$  values ( $>0.99$ ).

Total organic carbon (TOC) of dye samples was tested by a TOC analyzer (Aurora 1030D, O.I., College Station, Texas, USA). Fe(II) concentrations in dye samples were determined spectrophotometrically using the ferrozine method (Gibbs, 1976). The concentration of total soluble Fe (Fe<sub>T</sub>) in dye samples was quantified with an inductive coupled plasma emission spectrometer (OPTIMA 7000DV, PerkinElmer, Waltham, Massachusetts, USA).

## 2. Results

### 2.1. Characterization of nZVI

The BET surface area of nZVI was 15.7 m<sup>2</sup>/g, and the average pore width and pore volume of agglomerated nZVI were

1.426 nm and 0.07 m<sup>3</sup>/g, as determined using the Autosorb-iQ surface analyzer. The BET surface area of nZVI is half of the value (33.5 m<sup>2</sup>/g) reported by Wang and Zhang (1997), but is consistent with the value (15.524 m<sup>2</sup>/g) reported by Taha and Ibrahim (2014). A TEM image of the synthesized nZVI is shown in Fig. 2a, in which perfectly spherical, black nZVI particles ca. 40–70 nm in diameter can be observed; however, because the synthesized nZVI particles agglomerate when not used, an accurate measurement of the diameter of the individual particles was not possible in this study. Nevertheless, the diameter can be calculated to be 48.6 nm from the BET surface area using the equation from Taha and Ibrahim (2014), indicating the formation of smaller particles than previously reported (Joo et al., 2004; Wang and Zhang, 1997). The reduced size of the nZVI particles indicates that the presence of starch in the nZVI preparation process dispersed the nZVI particles in solution to give rise to smaller nZVI particles. Based on the XRF analysis of nZVI (Fig. 2b), the elemental composition of nZVI was determined to be 99.71% Fe and 0.134% Cl, indicating that a small amount of Cl<sup>−</sup> ions in the solution was absorbed onto the nZVI during preparation. It should be noted that XRF could not be used to determine the presence of oxygen because of the low fluorescence quantum yield of light elements. Therefore, the elemental composition of nZVI determined from XRF may have some errors. However, it is believed that oxygen would be present in very small proportions because the production of nZVI was performed under anaerobic conditions.

### 2.2. Kinetics of dyes removal by nZVI and MW–nZVI

Typical calibration data for investigating the kinetics of dye removal are shown in Fig. 3. The efficiency of the dye removal using only nZVI increased gradually with increasing contact time. During the initial 15 min (first stage), the dyes were rapidly discolored with a high probability of the adsorption of organic molecules onto the nZVI surface and the reduction of the chromophoric group of the organic molecules in the aqueous phase. The reaction involving the dissolution of ferrous ions of nZVI and electron transfer has been proved to be a fast process in a previous study (Shu et al., 2007). After complete mixing of nZVI and the dye solution, most of the active surface of nZVI was occupied by dye molecules; thus, the reaction rate slowed down and approached equilibrium,

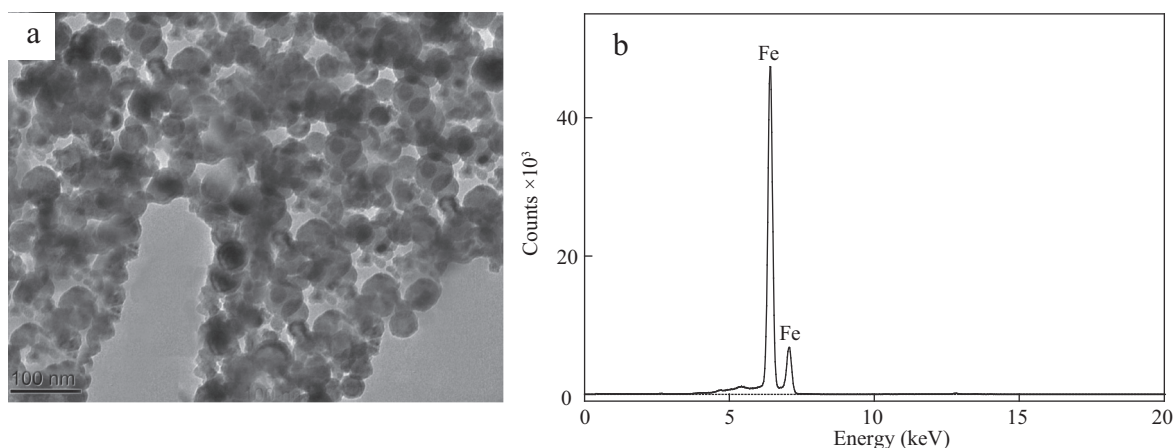


Fig. 2 – Transmission electron microscopy image (a) and X-ray fluorescence spectrum (b) of synthesized nanoscale zero-valent iron.

as observed for the last 15 min of the overall reaction time of 30 min. It is evident from Fig. 3 that nZVI was more effective for the removal of Blue than for Yellow, which is attributed primarily to the larger number of organic groups present in a molecule of Yellow compared to a molecule of Blue; thus, the former requires more nZVI to be degraded.

The use of MW radiation in combination with nZVI markedly increased the dye-removal rate and efficiency in both cases. When 50 mg/L Blue solution was subjected to treatment with MW–nZVI, as shown in Fig. 4, the maximum Blue removal efficiency achieved after 5 min was 56.5% and 81.4% using nZVI content ( $C_{Fe}$ ) 0.1 and 0.2 g/L at pH 7.0 and MP 450 W, respectively. These values are respectively 21.1% and 19.9% higher than the dye-removal efficiency achieved with nZVI alone in 30 min. When the MP was increased from 450 to 900 W, the maximum removal efficiency increased from 56.5% to 66% for  $C_{Fe}$  = 0.1 g/L and from 80.9% to 90.2% for  $C_{Fe}$  = 0.2 g/L. The trends observed for the removal of Yellow with MW–nZVI (Fig. 5) were similar to those observed for Blue. Using  $C_{Fe}$  = 0.1 and 0.3 g/L, the maximum removal efficiencies

of 60 mg/L Yellow were 40.4% and 64.8% at pH 7.0 and MP 450 W, which were achieved within 5 min, representing impressive enhancements of 27.3% and 28.9% relative to that achieved with only nZVI in 30 min. Furthermore, increasing the MP from 450 to 900 W could only enhance the removal efficiency of Yellow from 40.4% to 50.0% for  $C_{Fe}$  = 0.1 g/L and from 60.0% to 66.7% for  $C_{Fe}$  = 0.3 g/L. It was shown that the removal efficiency increased nonlinearly with increasing MP. Hence, the dominant factor influencing dye removal was the nZVI loading, whereas the MW primarily exerted an enhancement effect.

### 2.3. Effect of pH on dye removal by nZVI and MW–nZVI

The effect of pH on the dye removal efficiency was evaluated. The data in Fig. 3 show that increasing the pH resulted in a decrease in the removal efficiency for both Blue and Yellow. The maximum efficiency for removal for 50 mg/L Blue utilizing  $C_{Fe}$  = 0.2 g/L declined from 67.5% at pH = 5.0 to 48.9% at pH = 9.0, and the maximum efficiency for the

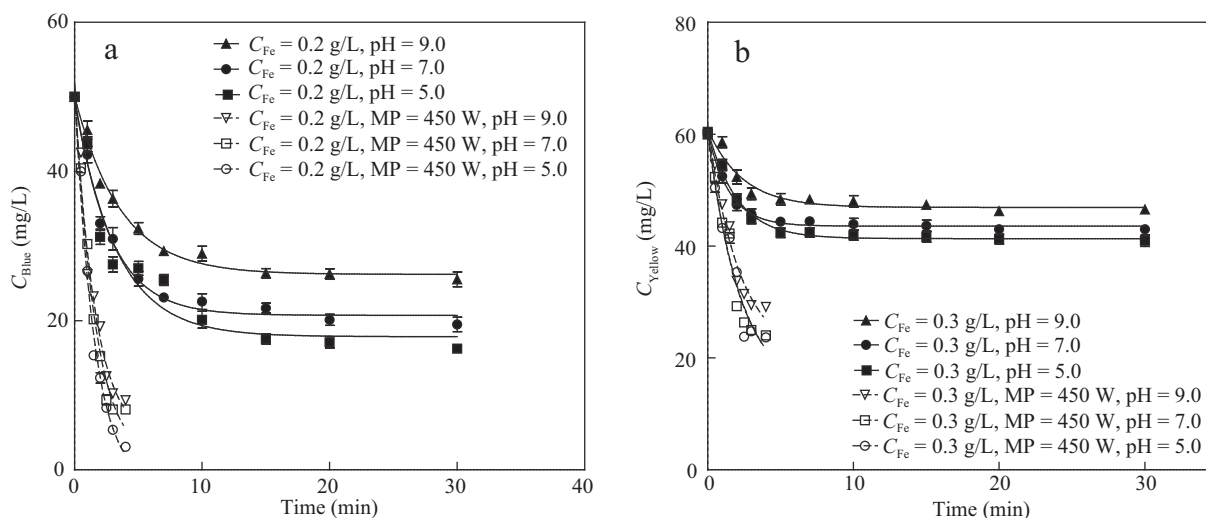
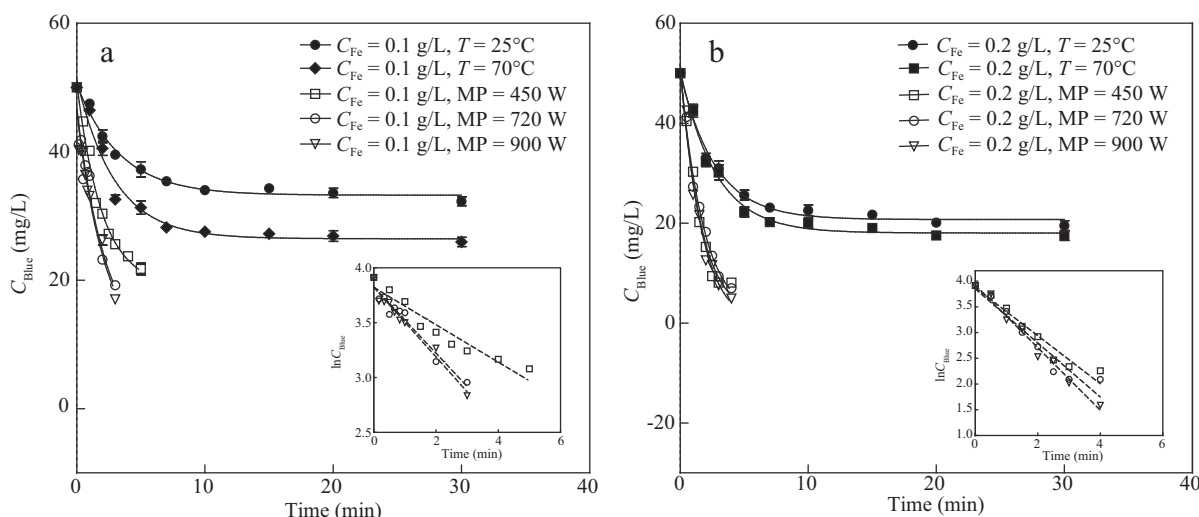


Fig. 3 – Nonlinear regression for kinetics of Solvent Blue 36 (Blue, a) and Reactive Yellow (Yellow, b) removal using only nanoscale zero-valent iron or microwave radiation in combination with nanoscale zero-valent iron.



**Fig. 4 – Nonlinear regression (solid lines) for kinetics of Blue removal using only nanoscale zero-valent iron at various temperatures at pH = 7.0 and using MW-nZVI at various microwave output power,  $C_{Fe} = 0.1$  g/L (a) and 0.2 g/L (b) at pH = 7.0. Pseudo first-order model (dotted lines) for the kinetics of Blue removal by microwave radiation in combination with nanoscale zero-valent iron at pH = 7.0.**

removal of 60 mg/L Yellow using  $C_{Fe} = 0.3$  g/L decreased from 31.8% at pH = 5.0 to 22.9% at pH = 9.0. In addition to the effects of nZVI loading and MW power on dye removal, the effect of pH on the dye-removal efficiency was also investigated (Fig. 3). At MP = 450 W, the maximum removal efficiency of Blue using  $C_{Fe} = 0.2$  g/L achieved in 5 min decreased from 93.8% at pH = 5.0 to 80.9% at pH = 9.0, and the maximum removal efficiency of Yellow using  $C_{Fe} = 0.3$  g/L achieved in 5 min decreased from 59.9% at pH = 5.0 to 51.5% at pH = 9.0.

Increasing the pH was evidently an unfavorable factor for dye removal in this study, which is similar to the trend observed for Methyl Orange removal using nZVI (Fan et al.,

2009) and for nitrate removal using nZVI (Yang and Lee, 2005). The faster corrosion of nZVI at lower pH leads to the generation of more hydroxyl radicals in the solution, with the consequent degradation of more dye molecules and higher dye-removal efficiency. Additionally, the point of zero charge of nZVI was determined to be 8.0 by Li et al. (2006); therefore, the surface of nZVI is positively charged at pH > 8.0, and can thus attract negatively charged amine groups in the dye molecules, leading to the better adsorption of the dyes on the surface of nZVI. At pH < 8.0, the surface of nZVI is negatively charged, which affects the adsorption of the dyes on its surface.

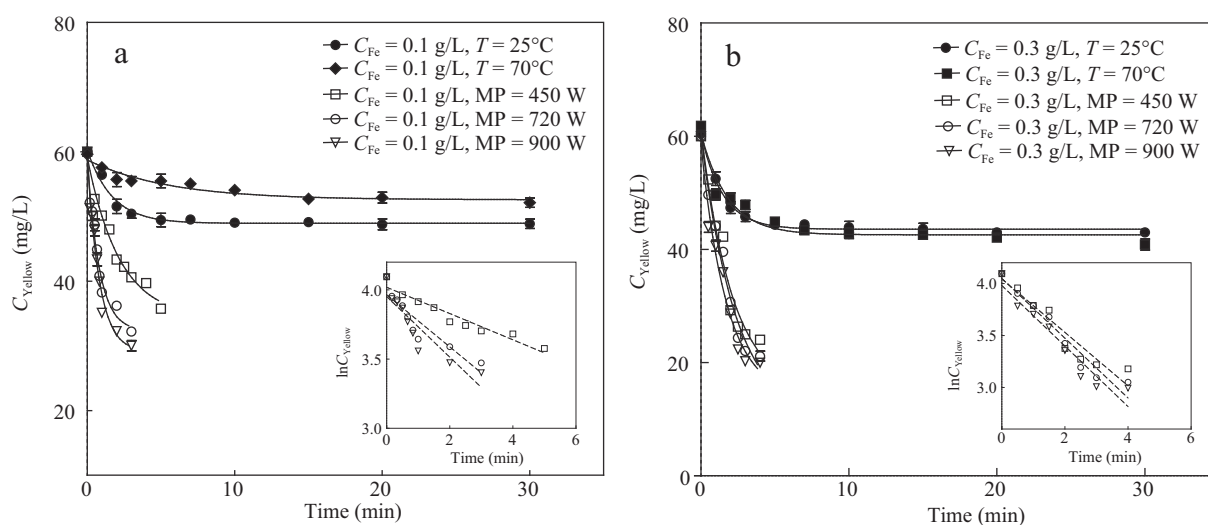


**Fig. 5 – Nonlinear regression (solid lines) for kinetics of Yellow removal using only nanoscale zero-valent iron at various temperatures at pH = 7.0 and using (MW-nZVI) microwave radiation in combination with nanoscale zero-valent iron (MW-nZVI) at various microwave output power,  $C_{Fe} = 0.1$  g/L (a) and 0.3 g/L (b) at pH = 7.0. Pseudo first-order model (dotted lines) for the kinetics of Yellow removal by MW-nZVI at pH = 7.0.**



## 2.4. TOC removal by nZVI and MW–nZVI

The intermediates during dye degradation may have no contribution to the absorbance at the studied wavelengths, while TOC levels in the solutions can be used to qualify the amount of organics. Therefore, the removal efficiencies of TOC were simultaneously measured at varying pH. It can be seen in Fig. 6 that the maximum TOC removal efficiency by nZVI was 25.6% for Blue (20.3% for Yellow) after 30 min at pH 5.0, and the maximum TOC removal efficiency by MW–nZVI was 60.2% for Blue (41.5% for Yellow) after 5 min at pH = 5.0. It was evident in both cases that the use of MW radiation markedly increased the TOC efficiency (by ca. 25%) and the TOC removal efficiency was lower than the dye degradation efficiency (by ca. 20%). The results further indicated that the dyes were degraded in the nZVI or MW–nZVI systems by producing a number of intermediates prior to mineralization, and the use of MW radiation dramatically enhanced the mineralization efficiency.

## 2.5. Formation of iron species in nZVI and MW–nZVI systems

In the process of dye degradation by nZVI or MW–nZVI, iron species, including ferrous iron and ferric iron, can be formed via the two-electron transfer between nZVI and oxygen. To verify the mechanism of dye degradation, the concentrations of Fe(II) and Fe<sub>T</sub> during the Blue removal were determined simultaneously. The concentration of Fe(II) in the system with  $C_{Fe} = 0.2$  g/L was measured as 0.120, 0.013, and 0.008 mmol/L after 30 min at pH 5.0, 7.0, and 9.0, respectively, while the concentration of Fe(II) in the system with  $C_{Fe} = 0.2$  g/L and MP = 450 W was markedly reduced to 0.082, 0.0017, and 0.0002 mmol/L after 5 min at pH 5.0, 7.0, and 9.0, respectively, indicating that the corrosion of nZVI was faster at lower pH and the reaction of Fe(II) with oxygen to produce Fe(III) and H<sub>2</sub>O<sub>2</sub> in the presence of MW radiation was faster than that in the absence of MW radiation. However, the concentration of

Fe<sub>T</sub> had the opposite tendency after the use of MW radiation. The higher residual Fe<sub>T</sub> at  $C_{Fe} = 0.2$  g/L and MP = 450 W (0.242, 0.138 and 0.091 mmol/L after 5 min at pH 5.0, 7.0, and 9.0) compared to that at  $C_{Fe} = 0.2$  g/L (0.154, 0.042 and 0.025 mmol/L after 5 min at pH 5.0, 7.0, and 9.0) was attributed to the fast corrosion of nZVI in the presence of MW radiation.

## 3. Discussion

### 3.1. Kinetic model for dye removal by nZVI and MW–nZVI

To describe the kinetics of dye removal by nZVI and MW–nZVI, the following empirical equation was used (Shu et al., 2007):

$$C = (C_0 - C_e) \times \sigma \times e^{-k_e t} + C_e \quad (2)$$

where,  $C$  (mg/L) is the concentration of the dye at reaction time  $t$ ,  $C_0$  (mg/L) is the initial concentration of the dye,  $C_e$  (mg/L) is the concentration of the dye when the reaction reaches equilibrium,  $k_e$  (sec<sup>-1</sup>) indicates the empirical rate constant for dye-removal kinetics, and  $\sigma$  denotes the variation coefficient, which was determined to be 1 by Fan et al. (2009).

The half-life ( $t_{1/2}$ , sec) of the dye can be expressed by the following equation:

$$t_{1/2} = \frac{\ln 2}{k} \quad (3)$$

Using nonlinear regression, a summary of the constants obtained ( $C_e$ ,  $k_e$ , and  $t_{1/2}$ ) for dye degradation kinetics based on different experimental data is given in Table 1. The  $r^2$  value ranged from 0.918 to 0.994, indicating good agreement between the empirical equation (Eq. (2)) and the observed data. The good fits of the kinetic models using different experimental variables are shown in Figs. 3–5. Variations of  $C_e$  with MP for different dyes and pH = 7.0 with different nZVI loadings are consistent with the experimental results demonstrating that MW radiation effectively enhanced the dye-removal efficiency, and that increasing the MP did not linearly increase the removal efficiency. Additionally, when more nZVI was loaded into the dye solutions, the enhancement in the dye-removal efficiency following MW radiation of the system was much higher. This result also indicated that, in this case, the dominant factor influencing the dye removal was nZVI, and MW radiation promoted dye removal by nZVI.

The kinetics of dye removal by MW–nZVI could be described using the pseudo first-order model (Figs. 4 and 5) with the  $r^2$  value ranging from 0.829 to 0.984 (Table 2). The rate constants  $k_1$  increased with increasing nZVI dosage and MW power, and with the same dosage of nZVI and MW power, the rate constants  $k_1$  for Blue were higher than for Yellow. However, the kinetics of dye removal by nZVI without MW radiation did not comply with the pseudo first-order model (figures were not shown), which is consistent with studies by Yang and Lee (2005) and Wang et al. (2006) and inconsistent with studies from Nam and Tratnyek (2000), Bigg and Judd (2001), and Epolito et al (2008).

### 3.2. Role of MW radiation in dye removal

It was found herein that the combination of MW radiation and nZVI was useful for achieving higher dye decolorization efficiency in a shorter duration than that achieved with only

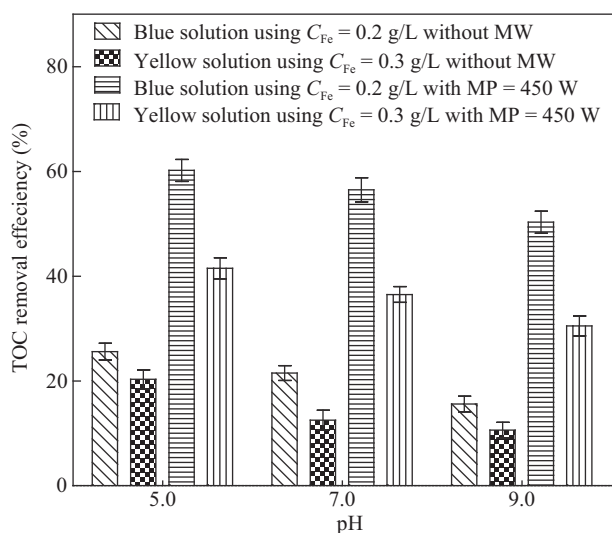


**Fig. 6 – TOC removal efficiency of dye solutions using nanoscale zero-valent iron (nZVI) and microwave radiation in combination with nanoscale zero-valent iron at various pH levels.**

**Table 1 – Parameters for empirical kinetics model.**

Experimental variables						Empirical kinetics			
Dyes	C <sub>Fe</sub> (g/L)	T (°C)	pH	Time (min)	MP (W)	C <sub>e</sub> (mg/L)	k <sub>e</sub> (sec <sup>-1</sup> )	t <sub>1/2</sub> (sec)	r <sup>2</sup>
Blue	0.1	25	7.0	30	0	33.2	4.99 × 10 <sup>-3</sup>	139	0.986
	0.1	70	7.0	30	0	26.5	5.64 × 10 <sup>-3</sup>	122.8	0.974
	0.1	65	7.0	5	450	19.1	8.58 × 10 <sup>-3</sup>	80.8	0.987
	0.1	71	7.0	3	720	8.13	7.09 × 10 <sup>-3</sup>	97.7	0.935
	0.1	78	7.0	3	900	7.90	7.09 × 10 <sup>-3</sup>	94.8	0.951
	0.2	25	7.0	30	0	20.7	6.09 × 10 <sup>-3</sup>	113.8	0.991
	0.2	70	7.0	30	0	18.0	6.04 × 10 <sup>-3</sup>	114.8	0.990
	0.2	66	7.0	5	450	1.87	9.18 × 10 <sup>-3</sup>	75.5	0.986
	0.2	73	7.0	3	720	1.31	10.4 × 10 <sup>-3</sup>	66.9	0.985
	0.2	79	7.0	3	900	0.79	10.1 × 10 <sup>-3</sup>	69.0	0.981
	0.2	25	5.0	30	0	17.9	5.09 × 10 <sup>-3</sup>	136.2	0.954
	0.2	25	9.0	30	0	26.2	4.70 × 10 <sup>-3</sup>	147.6	0.990
	0.2	65	5.0	5	450	0.893	10.9 × 10 <sup>-3</sup>	63.5	0.989
	0.2	66	9.0	5	450	4.10	10.4 × 10 <sup>-3</sup>	66.9	0.985
Yellow	0.1	25	7.0	30	0	52.6	3.04 × 10 <sup>-3</sup>	228.1	0.918
	0.1	70	7.0	30	0	49.0	9.98 × 10 <sup>-3</sup>	69.5	0.979
	0.1	65	7.0	5	450	34.3	7.66 × 10 <sup>-3</sup>	90.5	0.983
	0.1	69	7.0	3	720	32.3	20.8 × 10 <sup>-3</sup>	33.4	0.972
	0.1	78	7.0	3	900	29.1	20.4 × 10 <sup>-3</sup>	34.0	0.971
	0.3	25	7.0	30	0	43.6	11.4 × 10 <sup>-3</sup>	61.1	0.994
	0.3	70	7.0	30	0	42.6	9.29 × 10 <sup>-3</sup>	74.6	0.941
	0.3	65	7.0	5	450	14.4	7.79 × 10 <sup>-3</sup>	89.0	0.962
	0.3	70	7.0	3	720	9.60	7.05 × 10 <sup>-3</sup>	98.3	0.980
	0.3	78	7.0	3	900	14.0	9.58 × 10 <sup>-3</sup>	72.4	0.973
	0.3	25	5.0	30	0	41.3	8.38 × 10 <sup>-3</sup>	82.7	0.990
	0.3	25	9.0	30	0	46.9	7.00 × 10 <sup>-3</sup>	147.6	0.947
	0.3	65	5.0	5	450	12.7	7.04 × 10 <sup>-3</sup>	98.5	0.957
	0.3	66	9.0	5	450	20.3	7.69 × 10 <sup>-3</sup>	90.2	0.969

C<sub>Fe</sub>: nZVI content; T: temperature; MP: output power of microwave.

nZVI. The rapid, selective, and three-dimensional MW heating sharply elevated the temperature of the dye solutions with different nZVI loadings (Fig. 7), and the final temperature of the dye solutions was ca. 70°C (Table 1), indicating that the nZVI loading did not significantly affect the increase in the solution temperature. Nevertheless, it cannot be conclusively stated that nZVI was not a significant MW-absorbing material considering the small quantity of nZVI used in this study. It can only be deduced that the dominant MW-absorbing material in this system was water. To investigate the effect of temperature on dye removal by nZVI, several experiments were performed at different temperatures (25 and 70°C) in a thermostatic magnetic mixer (Figs. 4 and 5). Although the dye-removal efficiency increased slightly with temperature, this increase was far less than the efficiency achieved with MW thermal radiation. This implies that the rapid and selective heating of the dispersant (water in this case) by MW radiation was not the dominant mechanism for dye removal, which was consistent with the research by Horikoshi and Serpone (2014). Previous studies (Horikoshi et al., 2004a;

Jones et al., 2002; Liu et al., 2004; Lü et al., 2009) showed that hot spots were induced in the solutions when MW-absorbing materials such as activated carbon and TiO<sub>2</sub> were added to the MW medium. These hot spots may not induce an apparent increase in the temperature but may produce analogous plasmas around the hot spots (Horikoshi et al., 2004a), accelerating the degradation of target pollutants (Horikoshi et al., 2002). Meanwhile, although the quantized energy of MW radiation (10<sup>-6</sup>–10<sup>-3</sup> eV), which is much less than that of a chemical bond (10<sup>0</sup>–10<sup>1</sup> eV), cannot directly induce breakage of the chemical bonds (Müller et al., 2003), MW radiation can cause vibration or rotation of the chemical bonds, and hence weaken them and reduce the activation energy during the reaction with nZVI. Another possible explanation is that MW radiation may disrupt the hydrogen bonding of water molecules, thus activating them and promoting the desorption of water molecules from the surface of nZVI, increasing the surface activity of nZVI toward dye molecules. It was also revealed that the use of MW radiation could accelerate the corrosion of nZVI and the reaction of Fe(II) with oxygen to

**Table 2 – Parameters of pseudofirst-order model for dye removal by microwave radiation in combination with nanoscale zero-valent iron at pH = 7.0.**

C <sub>Fe</sub> (g/L)	Blue						Yellow					
	0.1			0.2			0.1			0.3		
k <sub>1</sub> × 10 <sup>-3</sup> (sec <sup>-1</sup> )	2.84	5.04	5.29	7.78	8.76	10.1	1.58	3.13	3.65	4.28	4.79	4.85
r <sup>2</sup>	0.920	0.954	0.970	0.946	0.927	0.984	0.929	0.836	0.829	0.910	0.946	0.928

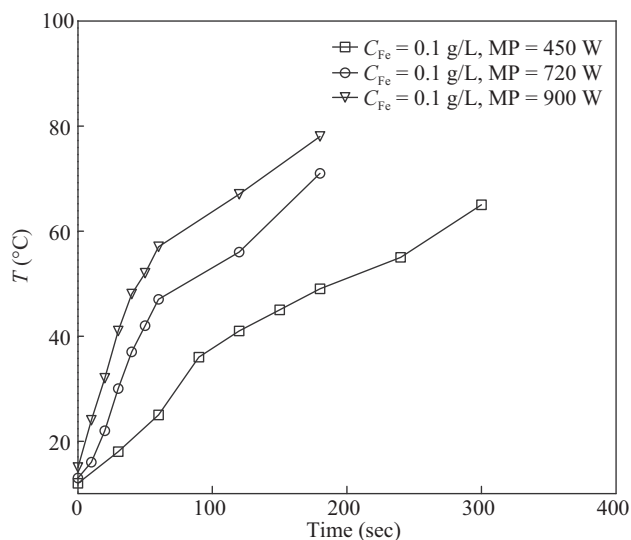


**Fig. 7 – Elevated temperature curve for Blue removal by  $C_{Fe} = 0.1$  g/L and different output power of microwave (450 W, 720 W and 900 W) at pH = 7.0.**

produce the Fe(III) and  $H_2O_2$ , and enhance the degradation of dyes as a consequence.

#### 4. Conclusions

The rapid and effective removal of dyes (Solvent Blue 36 and Reactive Yellow K-RN) by MW-nZVI under different experimental conditions was demonstrated herein. MW radiation significantly enhanced the degradation of the dyes and the mineralization efficiency in the presence of nZVI in 5 min. Increasing the pH decreased the efficiency of dye removal in the presence of both nZVI as well as with MW-nZVI; however, the dye-removal efficiency did not increase linearly in response to MP. Both the kinetics of dye removal by nZVI and by MW-nZVI could be described by an empirical equation. However, the pseudo-first-order model was only suitable for the kinetics of dye removal by MW-nZVI.

Although it has been concluded that the multiple actions of MW radiation may be the reaction mechanism for dye removal (as determined by eliminating the effect of rapid and selective heating of MW radiation on dye removal and accelerating the reaction of Fe(II) with oxygen to produce the Fe(III) and  $H_2O_2$ ), the pathways for the degradation of dyes and a detailed understanding of the reactions between the dyes and nZVI under MW radiation were not elucidated in this study. These studies are currently underway and will be reported in a future paper.

#### Acknowledgment

This work was supported by the Postdoctoral Science Foundation of China (No. 2013M531602), the Independent Innovation Foundation of Shandong University (No. IIFSDU 2012GN007), and the Shandong Post-Doctoral Science Foundation (No. 201202017).

#### REFERENCES

- Bigg, T., Judd, S., 2001. Kinetics of reductive degradation of azo dye by zero-valent iron. *Process Saf. Environ.* 79 (5), 297–303.
- Bokare, A.D., Chikate, R.C., Rode, C.V., Paknikar, K.M., 2008. Iron-nickel bimetallic nanoparticles for reductive degradation of azo dye Orange G in aqueous solution. *Appl. Catal. B Environ.* 79 (3), 270–278.
- Cao, J.S., Wei, L.P., Huang, Q.G., Wang, L.S., Han, S.K., 1999. Reducing degradation of azo dye by zero-valent iron in aqueous solution. *Chemosphere* 38 (3), 565–571.
- Chang, M.C., Shu, H.Y., Yu, H.H., Sung, Y.C., 2006. Reductive decolorization and total organic carbon reduction of the diazo dye CI Acid Black 24 by zero-valent iron powder. *J. Chem. Technol. Biotechnol.* 81 (7), 1259–1266.
- Comparelli, R., Fanizza, E., Curri, M.L., Cozzoli, P.D., Mascolo, G., Agostiano, A., 2005. UV-induced photocatalytic degradation of azo dyes by organic-capped ZnO nanocrystals immobilized onto substrates. *Appl. Catal. B Environ.* 60 (1–2), 1–11.
- Epollito, W.J., Yang, H., Bottomley, L.A., Pavlostathis, S.G., 2008. Kinetics of zero-valent iron reductive transformation of the anthraquinone dye Reactive Blue 4. *J. Hazard. Mater.* 160 (2–3), 594–600.
- Fan, J., Guo, Y.H., Wang, J.J., Fan, M.H., 2009. Rapid decolorization of azo dye methyl orange in aqueous solution by nanoscale zerovalent iron particles. *J. Hazard. Mater.* 166 (2–3), 904–910.
- Feng, W., Nansheng, D., Helin, H., 2000. Degradation mechanism of azo dye CI reactive red 2 by iron powder reduction and photooxidation in aqueous solutions. *Chemosphere* 41 (8), 1233–1238.
- Fu, J., Xu, Z., Li, Q.-S., Chen, S., An, S.Q., Zeng, Q.F., et al., 2010. Treatment of simulated wastewater containing Reactive Red 195 by zero-valent iron/activated carbon combined with microwave discharge electrodeless lamp/sodium hypochlorite. *J. Environ. Sci.* 22 (4), 512–518.
- Gibbs, C.R., 1976. Characterization and application of ferrozine iron reagent as a ferrous iron indicator. *Anal. Chem.* 48 (8), 1197–1201.
- Gromboni, C.F., Kamogawa, M.Y., Ferreira, A.G., Nóbrega, J.A., Nogueira, A.R.A., 2007. Microwave-assisted photo-Fenton decomposition of chlorfenvinphos and cypermethrin in residual water. *J. Photochem. Photobiol. A Chem.* 185 (1), 32–37.
- Gupta, V.K., Jain, R., Mittal, A., Saleh, T.A., Nayak, A., Agarwal, S., et al., 2012. Photo-catalytic degradation of toxic dye amaranth on  $TiO_2$ /UV in aqueous suspensions. *Mater. Sci. Eng. C* 32 (1), 12–17.
- Horikoshi, S., Serpone, N., 2014. On the influence of the microwaves' thermal and non-thermal effects in titania photoassisted reactions. *Catal. Today* 224, 225–235.
- Horikoshi, S., Hidaka, H., Serpone, N., 2002. Environmental remediation by an integrated microwave/UV-illumination method. 1. Microwave-assisted degradation of rhodamine-B dye in aqueous  $TiO_2$  dispersions. *Environ. Sci. Technol.* 36 (6), 1357–1366.
- Horikoshi, S., Hidaka, H., Serpone, N., 2004a. Environmental remediation by an integrated microwave/UV illumination technique: VI. A simple modified domestic microwave oven integrating an electrodeless UV-Vis lamp to photodegrade environmental pollutants in aqueous media. *J. Photochem. Photobiol. A Chem.* 161 (2–3), 221–225.
- Horikoshi, S., Hojo, F., Hidaka, H., Serpone, N., 2004b. Environmental remediation by an integrated microwave/UV illumination technique. 8. fate of carboxylic acids, aldehydes, alkoxy carbonyl and phenolic substrates in a microwave radiation field in the presence of  $TiO_2$  particles under UV irradiation. *Environ. Sci. Technol.* 38 (7), 2198–2208.
- Jones, D.A., Lelyveld, T.P., Mavrofidis, S.D., Kingman, S.W., Miles, N.J., 2002. Microwave heating applications in

- environmental engineering—a review. *Resour. Conserv. Recycl.* 34 (2), 75–90.
- Joo, S.H., Feitz, A.J., Waite, T.D., 2004. Oxidative degradation of the carbothioate herbicide, molinate, using nanoscale zero-valent iron. *Environ. Sci. Technol.* 38 (7), 2242–2247.
- Jou, C.-J., 2008. Degradation of pentachlorophenol with zero-valence iron coupled with microwave energy. *J. Hazard. Mater.* 152 (2), 699–702.
- Klán, P., Vavrik, M., 2006. Non-catalytic remediation of aqueous solutions by microwave-assisted photolysis in the presence of  $\text{H}_2\text{O}_2$ . *J. Photochem. Photobiol. A Chem.* 177 (1), 24–33.
- Krissanasaraanee, M., Wongkasemjit, S., Cheetham, A.K., Eder, D., 2010. Complex carbon nanotube-inorganic hybrid materials as next-generation photocatalysts. *Chem. Phys. Lett.* 496 (1–3), 133–138.
- Lee, C.L., Jou, C.J.G., 2012. Degradation of chlorobenzene with microwave-aided zerovalent iron particles. *Environ. Eng. Sci.* 29 (6), 432–435.
- Lee, Y.C., Lo, S.L., Chiu, P.T., Chang, D.G., 2009. Efficient decomposition of perfluorocarboxylic acids in aqueous solution using microwave-induced persulfate. *Water Res.* 43 (11), 2811–2816.
- Lee, C.L., Jou, C.J., Wang, H.P., 2010. Enhanced degradation of chlorobenzene in aqueous solution using microwave-induced zero-valent iron and copper particles. *Water Environ. Res.* 82 (7), 642–647.
- Li, X.Q., Elliott, D.W., Zhang, W.X., 2006. Zero-valent iron nanoparticles for abatement of environmental pollutants: materials and engineering aspects. *Crit. Rev. Solid State Mater. Sci.* 31 (4), 111–122.
- Lin, Y.T., Weng, C.H., Chen, F.Y., 2008. Effective removal of AB24 dye by nano/micro-size zero-valent iron. *Sep. Purif. Technol.* 64 (1), 26–30.
- Liu, X.T., Quan, X., Bo, L.L., Chen, S., Zhao, Y.Z., 2004. Simultaneous pentachlorophenol decomposition and granular activated carbon regeneration assisted by microwave irradiation. *Carbon* 42 (2), 415–422.
- Liu, H., Li, G., Qu, J., Liu, H., 2007. Degradation of azo dye Acid Orange 7 in water by  $\text{Fe}^0$ /granular activated carbon system in the presence of ultrasound. *J. Hazard. Mater.* 144 (1–2), 180–186.
- Lü, S.S., Chen, X.G., Ye, Y., Yin, S.H., Cheng, J.P., Xia, M.S., 2009. Rice hull/ $\text{MnFe}_2\text{O}_4$  composite: preparation, characterization and its rapid microwave-assisted COD removal for organic wastewater. *J. Hazard. Mater.* 171 (1–3), 634–639.
- Mu, Y., Yu, H.Q., Zhang, S.J., Zheng, J.C., 2004. Kinetics of reductive degradation of Orange II in aqueous solution by zero-valent iron. *J. Chem. Technol. Biotechnol.* 79 (12), 1429–1431.
- Müller, P., Klán, P., Čírkva, V., 2003. The electrodeless discharge lamp: a prospective tool for photochemistry: part 4. Temperature and envelope material-dependent emission characteristics. *J. Photochem. Photobiol. A Chem.* 158 (1), 1–5.
- Nam, S., Tratnyek, P.G., 2000. Reduction of azo dyes with zero-valent iron. *Water Res.* 34 (6), 1837–1845.
- Oh, S.Y., Chiu, P.C., Kim, B.J., Cha, D.K., 2006. Enhanced reduction of perchlorate by elemental iron at elevated temperatures. *J. Hazard. Mater.* 129 (1–3), 304–307.
- Perey, J.R., Chiu, P.C., Huang, C.P., Cha, D.K., 2002. Zero-valent iron pretreatment for enhancing the biodegradability of azo dyes. *Water Environ. Res.* 74 (3), 221–225.
- Prasannakumar, B.R., Regupathi, I., Murugesan, T., 2009. An optimization study on microwave irradiated decomposition of phenol in the presence of  $\text{H}_2\text{O}_2$ . *J. Chem. Technol. Biotechnol.* 84 (1), 83–91.
- Remya, N., Lin, J.G., 2011a. Current status of microwave application in wastewater treatment—a review. *Chem. Eng. J.* 166 (3), 797–813.
- Remya, N., Lin, J.G., 2011b. Microwave-assisted carbofuran degradation in the presence of GAC, ZVI and  $\text{H}_2\text{O}_2$ : influence of reaction temperature and pH. *Sep. Purif. Technol.* 76 (3), 244–252.
- Shandong Environmental Protection Agency, 2006. The water pollutant discharge standard for South-to-North Water Transfer project in Shandong Province DB37/ 599–2006, Shandong.
- Shu, H.Y., Chang, M.C., Yu, H.H., Chen, W.H., 2007. Reduction of an azo dye Acid Black 24 solution using synthesized nanoscale zerovalent iron particles. *J. Colloid Interface Sci.* 314 (1), 89–97.
- Shu, H.Y., Chang, M.C., Chen, C.C., Chen, P.E., 2010. Using resin supported nano zero-valent iron particles for decoloration of Acid Blue 113 azo dye solution. *J. Hazard. Mater.* 184 (1–3), 499–505.
- Taha, M.R., Ibrahim, A.H., 2014. Characterization of nano zero-valent iron (nZVI) and its application in sono-Fenton process to remove COD in palm oil mill effluent. *J. Environ. Chem. Eng.* 2 (1), 1–8.
- Tichonovas, M., Krugly, E., Racys, V., Hippler, R., Kauneliene, V., Stasiulaitiene, I., et al., 2013. Degradation of various textile dyes as wastewater pollutants under dielectric barrier discharge plasma treatment. *Chem. Eng. J.* 229, 9–19.
- Wang, C.B., Zhang, W.X., 1997. Synthesizing nanoscale iron particles for rapid and complete dechlorination of TCE and PCBs. *Environ. Sci. Technol.* 31 (7), 2154–2156.
- Wang, W., Jin, Z.H., Li, T.L., Zhang, H., Gao, S., 2006. Preparation of spherical iron nanoclusters in ethanol–water solution for nitrate removal. *Chemosphere* 65 (8), 1396–1404.
- Yang, G.C.C., Lee, H.L., 2005. Chemical reduction of nitrate by nanosized iron: kinetics and pathways. *Water Res.* 39 (5), 884–894.
- Yang, Y., Wang, P., Shi, S., Liu, Y., 2009. Microwave enhanced Fenton-like process for the treatment of high concentration pharmaceutical wastewater. *J. Hazard. Mater.* 168 (1), 238–245.
- Zhang, H., Duan, L., Zhang, Y., Wu, F., 2005. The use of ultrasound to enhance the decolorization of the CI acid Orange 7 by zero-valent iron. *Dyes Pigments* 65 (1), 39–43.
- Zhang, X.W., Li, G.T., Wang, Y.Z., 2007. Microwave assisted photocatalytic degradation of high concentration azo dye Reactive Brilliant Red X-3B with microwave electrodeless lamp as light source. *Dyes Pigments* 74 (3), 536–544.
- Zhanqi, G., Shaogui, Y., Na, T., Cheng, S., 2007. Microwave assisted rapid and complete degradation of atrazine using  $\text{TiO}_2$  nanotube photocatalyst suspensions. *J. Hazard. Mater.* 145 (3), 424–430.





## Editorial Board of Journal of Environmental Sciences

### Editor-in-Chief

**X. Chris Le** University of Alberta, Canada

### Associate Editors-in-Chief

**Jiuhui Qu** Research Center for Eco-Environmental Sciences, Chinese Academy of Sciences, China  
**Shu Tao** Peking University, China  
**Nigel Bell** Imperial College London, UK  
**Po-Keung Wong** The Chinese University of Hong Kong, Hong Kong, China

### Editorial Board

#### Aquatic environment

**Baoyu Gao** Shandong University, China  
**Maohong Fan** University of Wyoming, USA  
**Chihpin Huang** National Chiao Tung University, Taiwan, China  
**Ng Wun Jern** Nanyang Environment & Water Research Institute, Singapore  
**Clark C. K. Liu** University of Hawaii at Manoa, USA  
**Hokyong Shon** University of Technology, Sydney, Australia  
**Zijian Wang** Research Center for Eco-Environmental Sciences, Chinese Academy of Sciences, China  
**Zhiwu Wang** The Ohio State University, USA  
**Yuxiang Wang** Queen's University, Canada  
**Min Yang** Research Center for Eco-Environmental Sciences, Chinese Academy of Sciences, China  
**Zhifeng Yang** Beijing Normal University, China  
**Han-Qing Yu** University of Science & Technology of China, China

#### Terrestrial environment

**Christopher Anderson** Massey University, New Zealand  
**Zucong Cai** Nanjing Normal University, China  
**Xinbin Feng** Institute of Geochemistry, Chinese Academy of Sciences, China  
**Hongqing Hu** Huazhong Agricultural University, China  
**Kin-Che Lam** The Chinese University of Hong Kong, Hong Kong, China  
**Erwin Klumpp** Research Centre Juelich, Agrosphere Institute, Germany

#### Peijun Li

Institute of Applied Ecology, Chinese Academy of Sciences, China  
**Michael Schlöter** German Research Center for Environmental Health, Germany  
**Xuejun Wang** Peking University, China  
**Lizhong Zhu** Zhejiang University, China

#### Atmospheric environment

**Jianmin Chen** Fudan University, China  
**Abdelwahid Mellouki** Centre National de la Recherche Scientifique, France  
**Yujing Mu** Research Center for Eco-Environmental Sciences, Chinese Academy of Sciences, China  
**Min Shao** Peking University, China  
**James Jay Schauer** University of Wisconsin-Madison, USA  
**Yuesi Wang** Institute of Atmospheric Physics, Chinese Academy of Sciences, China  
**Xin Yang** University of Cambridge, UK

#### Environmental biology

**Yong Cai** Florida International University, USA  
**Henner Hollert** RWTH Aachen University, Germany  
**Jae-Seong Lee** Sungkyunkwan University, South Korea  
**Christopher Rensing** University of Copenhagen, Denmark  
**Bojan Sedmak** National Institute of Biology, Slovenia  
**Lirong Song** Institute of Hydrobiology, Chinese Academy of Sciences, China  
**Chunxia Wang** National Natural Science Foundation of China  
**Gehong Wei** Northwest A & F University, China

#### Daqiang Yin

Tongji University, China  
**Zhongtang Yu** The Ohio State University, USA

#### Environmental toxicology and health

**Jingwen Chen** Dalian University of Technology, China  
**Jianying Hu** Peking University, China  
**Guibin Jiang** Research Center for Eco-Environmental Sciences, Chinese Academy of Sciences, China  
**Sijin Liu** Research Center for Eco-Environmental Sciences, Chinese Academy of Sciences, China  
**Tsuyoshi Nakanishi** Gifu Pharmaceutical University, Japan

**Willie Peijnenburg** University of Leiden, The Netherlands  
**Bingsheng Zhou** Institute of Hydrobiology, Chinese Academy of Sciences, China

#### Environmental catalysis and materials

**Hong He** Research Center for Eco-Environmental Sciences, Chinese Academy of Sciences, China  
**Junhua Li** Tsinghua University, China  
**Wenfeng Shangguan** Shanghai Jiao Tong University, China  
**Ralph T. Yang** University of Michigan, USA

#### Environmental analysis and method

**Zongwei Cai** Hong Kong Baptist University, Hong Kong, China  
**Jiping Chen** Dalian Institute of Chemical Physics, Chinese Academy of Sciences, China  
**Minghui Zheng** Research Center for Eco-Environmental Sciences, Chinese Academy of Sciences, China  
**Municipal solid waste and green chemistry**  
**Pinjing He** Tongji University, China

### Editorial office staff

**Managing editor** Qingcai Feng  
**Editors** Zixuan Wang Suqin Liu Kuo Liu Zhengang Mao  
**English editor** Catherine Rice (USA)

# JOURNAL OF ENVIRONMENTAL SCIENCES

环境科学学报(英文版)

[www.jesc.ac.cn](http://www.jesc.ac.cn)

## Aims and scope

*Journal of Environmental Sciences* is an international academic journal supervised by Research Center for Eco-Environmental Sciences, Chinese Academy of Sciences. The journal publishes original, peer-reviewed innovative research and valuable findings in environmental sciences. The types of articles published are research article, critical review, rapid communications, and special issues.

The scope of the journal embraces the treatment processes for natural groundwater, municipal, agricultural and industrial water and wastewaters; physical and chemical methods for limitation of pollutants emission into the atmospheric environment; chemical and biological and phytoremediation of contaminated soil; fate and transport of pollutants in environments; toxicological effects of terrorist chemical release on the natural environment and human health; development of environmental catalysts and materials.

## For subscription to electronic edition

Elsevier is responsible for subscription of the journal. Please subscribe to the journal via <http://www.elsevier.com/locate/jes>.

## For subscription to print edition

China: Please contact the customer service, Science Press, 16 Donghuangchenggen North Street, Beijing 100717, China. Tel: +86-10-64017032; E-mail: [journal@mail.sciencep.com](mailto:journal@mail.sciencep.com), or the local post office throughout China (domestic postcode: 2-580).

Outside China: Please order the journal from the Elsevier Customer Service Department at the Regional Sales Office nearest you.

## Submission declaration

Submission of the work described has not been published previously (except in the form of an abstract or as part of a published lecture or academic thesis), that it is not under consideration for publication elsewhere. The publication should be approved by all authors and tacitly or explicitly by the responsible authorities where the work was carried out. If the manuscript accepted, it will not be published elsewhere in the same form, in English or in any other language, including electronically without the written consent of the copyright-holder.

## Editorial

Authors should submit manuscript online at <http://www.jesc.ac.cn>. In case of queries, please contact editorial office, Tel: +86-10-62920553, E-mail: [jesc@rcees.ac.cn](mailto:jesc@rcees.ac.cn). Instruction to authors is available at <http://www.jesc.ac.cn>.

## Journal of Environmental Sciences (Established in 1989) Volume 30 2015

<b>Supervised by</b>	Chinese Academy of Sciences	<b>Published by</b>	Science Press, Beijing, China
<b>Sponsored by</b>	Research Center for Eco-Environmental Sciences, Chinese Academy of Sciences		Elsevier Limited, The Netherlands
<b>Edited by</b>	Editorial Office of Journal of Environmental Sciences P. O. Box 2871, Beijing 100085, China Tel: 86-10-62920553; <a href="http://www.jesc.ac.cn">http://www.jesc.ac.cn</a> E-mail: <a href="mailto:jesc@rcees.ac.cn">jesc@rcees.ac.cn</a>	<b>Distributed by</b>	
		Domestic	Science Press, 16 Donghuangchenggen North Street, Beijing 100717, China Local Post Offices through China
		Foreign	Elsevier Limited <a href="http://www.elsevier.com/locate/jes">http://www.elsevier.com/locate/jes</a>
<b>Editor-in-chief</b>	X. Chris Le	<b>Printed by</b>	Beijing Beilin Printing House, 100083, China

CN 11-2629/X Domestic postcode: 2-580

Domestic price per issue RMB ¥ 110.00

ISSN 1001-0742

